Influence of an inert electrolyte on the morphology of quasi-two-dimensional electrodeposits

Pedro Pablo Trigueros, Francesc Sagués, and Josep Claret
Departament de Química Física, Facultat de Química, Universitat de Barcelona, c/Martí i Franqués 1, E08028-Barcelona, Catalonia, Spain
(Received 15 June 1993)

The influence of an inert electrolyte (sodium sulfate) on quasi-two-dimensional copper electrodeposition from a nondeaerated aqueous copper sulfate solution has been analyzed. The different morphologies for a fixed concentration of $CuSO_4$ have been classified in a diagram in terms of the applied potential and the inert electrolyte concentration. The main conclusion is the extension of the well-known Ohmic model for the homogeneous growth regime for copper sulfate solutions with small amounts of sodium sulfate. Moreover, we have observed the formation of fingerlike deposits at large applied potential and inert electrolyte concentration values, before hydrogen evolution becomes the main electrode reaction.

PACS number(s): 68.70.+w, 82.45.+z, 61.50.Cj

I. INTRODUCTION

It is well recognized that electrochemical deposition is a typical example of far from equilibrium growth phenomena [1,2]. In particular, quasi-two-dimensional electrodeposition is useful to analyze and discuss different pattern morphologies that can be obtained under nonequilibrium conditions. In such experiments, a metallic electrodeposit is grown from a thin layer of aqueous electrolyte solution containing the metal cation to be reduced. Actually, it has been clearly shown that the electrodeposit morphology depends on a series of experimental parameters such as cation concentration, applied potential difference, cell dimensions (mainly cell thickness and electrode separation), etc. [3–6].

However, the effect of the composition of the electrolyte solution on the quasi-two-dimensional electrodeposit morphology has not been widely studied. Restricting ourselves to nondeaerated aqueous electrolyte solutions, some aspects deserve special attention. First of all, one should consider the presence of chemically inactive electrolytes (inert electrolytes) which might affect the transport mechanism of the active cation from the bulk solution to the electrode surface. Second, chemically active electrolytes could modify the nature of the metal species in solution. This, for instance, would be the role of some complexing anions. Finally, the effect of organic additives (surface active compounds) on the morphology of these deposits is also an important question in this context.

In particular, the aim of this paper is to study the influence of an inert electrolyte on the deposit morphology. In this sense, we have chosen the simplest situation which consists in an electrolyte solution containing three different ions, i.e., an inert electrolyte with the same anion as the electroactive electrolyte. Following our past experience with zinc electrodeposition at constant potential difference between anode and cathode in a parallel cell from a $ZnSO_4$ solution [5,6], our first attempt was conducted with the system $ZnSO_4+Na_2SO_4$. Moreover, experimental conditions were selected in order to obtain homogeneous (dense parallel branched) patterns, whose steadily advancing front makes possible the reliable measurement of the most distinctive growth features of the metallic deposit. However, as also previously observed by Kahanda and Tomkiewicz [7], we found that hydrogen evolution was the main electrode reaction after small additions of sodium sulfate to a zinc sulfate solution (1 m*M* $Na_2SO_4+0.04M$ $ZnSO_4$). According to previous reports indicating that homogeneous patterns are also obtained in copper electrodeposition under similar experimental conditions [8,9], the system $CuSO_4+Na_2SO_4$ was finally chosen. Since copper is a more noble metal than zinc, a quite ample range of experimental conditions (constant applied voltage and inert electrolyte concentration) give rise to the characteristic homogeneous patterns. In addition, and as reported below, other morphologies different from homogeneous ones are also observed.

The natural way to look for distinctive effects of an inert electrolyte on the standard quasi-two-dimensional electrodeposition process is to characterize the different deposit structures and their associated dynamic transitions, obtained when appropriately varying the experimental conditions. This is accomplished here by first presenting in Sec. III a diagram of morphologies restricted, for simplicity, to a fixed concentration of the electroactive electrolyte. Actually, some of these morphologies turn out to be characteristic of the reference system, i.e., without inert species. However, and more important, we have also found other textures and morphological transitions, preliminarily interpreted in Sec. V, that, as far as we know, have never been reported before in standard references of quasi-two-dimensional copper electrodeposition. In between, in Sec. IV, an Ohmic model is used to describe the homogeneous growth mode under our particular experimental conditions. Finally, Sec. VI summarizes some conclusions.

II. EXPERIMENT

The experimental setup for electrodeposition experiments and data analysis has been described elsewhere

[5,6]. Time sequence images of the aggregates were digitized and processed to determine the growth velocity. This parameter has been measured as the displacement rate of the tips of the trees which determine the growing front of the deposit. The calculated values agree with those obtained by means of other methods, i.e., mean height vs time.

Conductivity measurements were made using a Radiometer CDM3 conductivity meter under the same experimental conditions as for the electrodeposition experiments.

In most experiments, a quasi-two-dimensional electrodeposition cell with a copper anode immersed in an anodic solution compartment external to the electrolyte thin layer has been used [6]. The cathode is a copper wire parallel to the anode; its diameter determines the thickness of the cell. Typical cell dimensions are cell thickness 105 μm, electrode separation 4 cm, and electrode length 11 cm.

Aggregates were grown at the cathode by imposing a constant potential difference (up to 30 V). Electrolyte solutions were prepared using ultrapure water supplied by a Millipore Milli Q system, and reagent grade cupric sulfate and sodium sulfate (Merck, p.a. grade). The purity of copper electrodes is 99.98%.

Electrodeposition experiments were performed at room temperature (20±1 °C).

The concentration effects on ion mobility were evaluated by means of the Debye-Huckel-Onsager theory [10]. Conductivity data of unsupported $CuSO_4$ solutions were taken from Miller *et al.* [11].

III. EXPERIMENTAL RESULTS

A. Diagram of morphologies

The different deposit morphologies are classified in the diagram of morphologies of Fig. 1, as a function of sodium sulfate concentration and applied potential values while keeping fixed the concentration of copper sulfate at 0.05*M*. Its dividing lines have been constructed after analyzing over 75 patterns corresponding to different experimental conditions conveniently scattered on the diagram. Only the first structure of the deposit up to approximately 5 mm is reported.

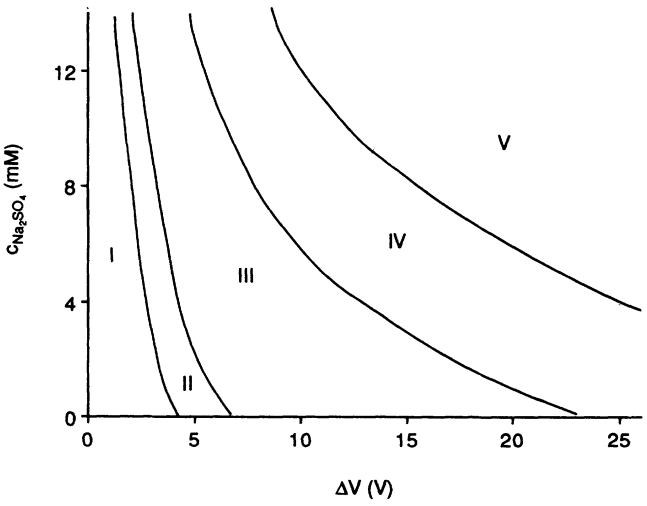

FIG. 1. Diagram of morphologies for copper electrodeposition from a 0.05*M* copper sulfate aqueous solution containing sodium sulfate. Zone I: compact; zone II: open fractal; zone III: homogeneous; zone IV: fingerlike morphologies. Zone V corresponds to hydrogen evolution.

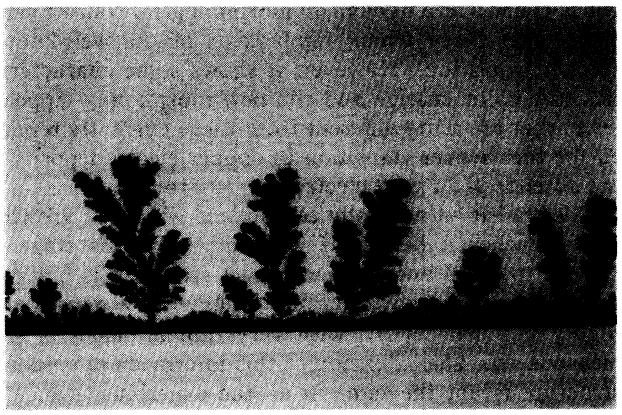

FIG. 2. Open fractal copper electrodeposit corresponding to zone II of the diagram of morphologies. The width of the picture corresponds to 23 mm. $\Delta V = 5$ V, $[Na_2SO_4] = 1$ m*M*.

In zone I, a compact and very poorly structured deposit is obtained (it only attains typical heights of 1 mm after two hours of electrodeposition). In zone II, the first structure is a red open fractal copper deposit (Fig. 2), whereas in zone III, we observe a reddish, metallic, homogeneous (dense parallel branched) pattern (Fig. 3). The number of trees increases with the inert electrolyte concentration and the applied potential. These two structures are similar to some others reported previously for copper electrodeposition in the absence of insert electrolyte at small cell thickness (less than 100 μm) [8]. At larger cell thickness, a black deposit is initially obtained, attributed to the formation of a cupric oxide layer on the copper deposit [12].

Under the experimental conditions corresponding to

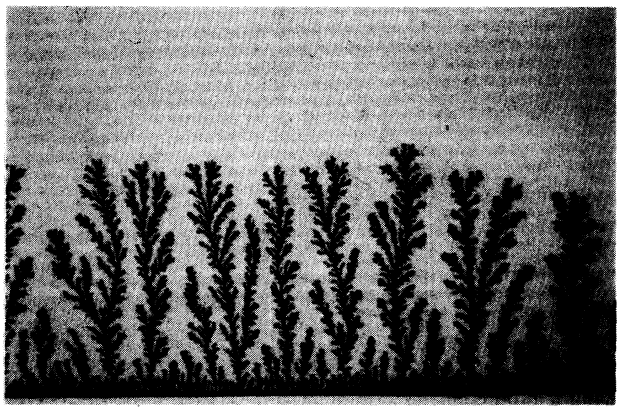

FIG. 3. Homogeneous copper electrodeposit corresponding to zone III of the diagram of morphologies. The width of the picture corresponds to 23 mm. $\Delta V = 5$ V, $[Na_2SO_4] = 4$ m*M*.

zones II and III, a dynamical morphological transition always takes place which reminds us of the well-known Hecker transition. However, it shows some characteristics (the color change and the new morphology appearance) that are quite different from those currently reported for the Hecker transition in copper electrodeposits in the absence of an inert electrolyte [12–14].

The transition normally takes place when the growing front reaches a height of 7–8 mm. At this stage, a change to a red and more compact structure is first observed, and afterwards, another change to a denser and highly ramified deposit with very thin branches is also clearly seen. The extension of this intermediate compact structure is not the same in all the experiments and, in some cases, it is even very short, but it is always observed before the formation of the last dense morphology.

Three properties of this last structure deserve special attention: (i) its dull and grey appearance with a nonmetallic aspect, (ii) the presence of some hydrogen bubbles without breaking the whole shape of the deposit, and (iii) the tips of the thin branches which form a very well-defined growing boundary in such a way that the deposit profile reminds us of the typical viscous fingering shapes, when observed at large length scales (Fig. 4). For this reason, this texture is hereafter referred as a finger-like morphology. When these fingers grow, they define a sort of front, with higher separation between fingers than between trees in a homogeneous pattern. At larger developments of finger patterns, a new transition to red open structures on the top of several fingers is clearly observed.

At higher inert electrolyte concentration and applied potential values (zone IV), the first structure of the deposit is the finger pattern (Fig. 5). Like homogeneous patterns, the number of fingers increases with the inert electrolyte concentration and the applied potential. Under the experimental conditions close to the transition between zones III and IV of the diagram of morphologies, a more complex pattern is observed in most cases. In these conditions, we can observe that the first portion of the deposit has the same fine structure as finger patterns, but its growing front is parallel to the cathode. Before the formation of fingers, the deposit morphology changes to a homogeneous structure, and its further evolution is as mentioned in the preceding paragraph. In zone V hydrogen evolution is the main electrode reaction and no deposit is obtained on the cathode.

FIG. 4. Complex pattern showing the dynamical transition from a homogeneous structure to a fingerlike texture. Notice that the fine structure of the first part of the deposit is the same as that of the fingerlike morphology. The width of the picture corresponds to 23 mm. $\Delta V=5$ V, $[Na_2SO_4]=6$ mM.

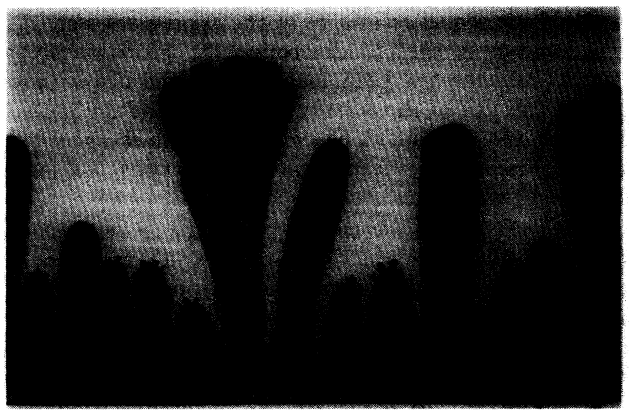

FIG. 5. Fingerlike copper electrodeposit corresponding to zone IV of the diagram of morphologies. The width of the picture corresponds to 23 mm. $\Delta V=25$ V, $[Na_2SO_4]=2$ mM.

Apart from the particular conditions under which the newly found fingerlike texture is observed as the dominant growth mode, it is worth noting that the deposit morphologies, although similar, are always affected by the presence of sodium sulfate. This is clearly evidenced when comparing with the structures obtained from standard copper electrodeposition conducted at the same applied potential values. As a general rule, the presence of the sodium sulfate renders the deposit better structured and, in particular, for homogeneous patterns, the growing front is also more sharply defined. Actually, this agrees with the previous observations by Kahanda and Tomkiewicz [7].

B. Current density vs time dependence

The temporal evolution of current density during copper electrodeposition under constant applied potential

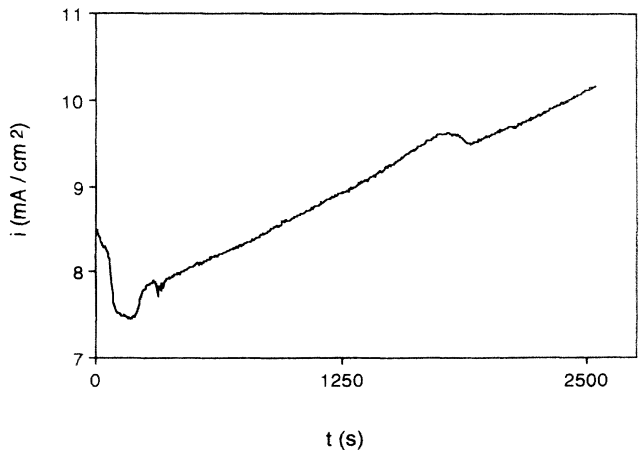

FIG. 6. Typical current density vs time plot for zone III of the diagram of morphologies. $\Delta V=7$ V, $[Na_2SO_4]=2$ mM.

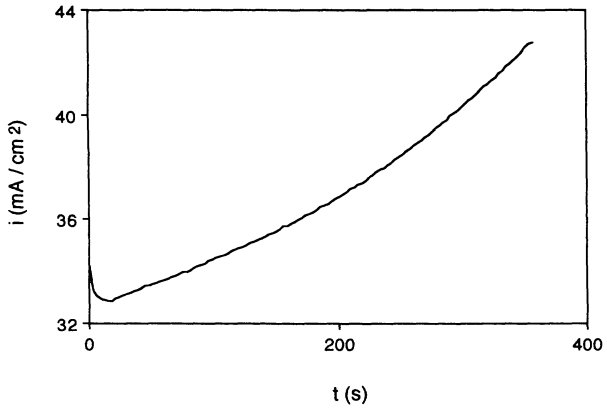

FIG. 7. Typical current density vs time plot for zone IV of the diagram of morphologies. $\Delta V=25$ V, $[Na_2SO_4]=1.75$ mM.

exhibits similar trends for the different morphologies.

A typical current density vs time plot for zone III is shown in Fig. 6, and clearly involves different stages. The first stage of this curve is a continuous decrease of current until a minimum value is reached. During this transient regime, which decreases when sodium sulfate concentration and applied potential increases, the cathode surface is covered by a stable deposit without irregularities. We can assign this behavior to nucleation processes involved in the first steps of the electrodeposition reaction, and we can refer to this time range as the induction time of the growth process. When the cathode surface is fully covered by a regular deposit and a homogeneous structure is formed, current density increases until the transition to a finger pattern takes place. At this moment, current falls down and attains a minimum value to rise again when the finger structure is formed and grows steadily. This last behavior is also observed under the experimental conditions close to the transition between zones III and IV. In this case, a current increase always accompanies the dynamic transition between the first fingerlike deposit and the homogeneous structure.

Figure 7 shows a typical current density vs time plot for zone IV of the diagram of morphologies. The absence of dynamical morphological transitions makes current continuously increase after the initial minimum value.

IV. A MODEL FOR HOMOGENEOUS PATTERN GROWTH

The formation of homogeneous patterns from an aqueous binary electrolyte solution has been explained by assigning to migration the major role on the transport of electroactive cations to the electrode surface [9,12,15,16]. Our aim, now, is to extend and test this Ohmic model for the growth of a homogeneous pattern in the presence of small concentrations of an inert electrolyte.

According to previous studies on the formation of homogeneous patterns [9,12,15,16], a model to analyze this growth mode may be formulated taking into account the following assumptions: (i) if the ionic migration towards the electrode surface is the limiting step of the process, the concentration of electroactive species on the electrode surface vanishes; (ii) copper electrodeposition is the only reaction on the cathode surface, and only takes place on the growing front of the deposit. This means that no current is flowing through the solution between the branches of the deposit, so that the concentration of electroactive cation (copper) is zero behind the growing front; (iii) the absence of electroactive cations (copper) between the branches of the deposit and the metallic nature of the filaments allows us to consider the zone between the cathode wire and the tips of the branches as an equipotential region; (iv) the electrolyte solution is stationary and uniform, and contributions from concentration layers of both electrodes are neglected. We consider that both the conductivity and the electric field are homogeneous along the cell solution. This supposition may be more realistic as inert electrolyte concentration is higher; and (v) electroneutrality is fulfilled through all the solution.

A material balance for the three ions of the system may be expressed by the following equations:

$$vC_{Cu}+\mu_{Cu}EC_{Cu}=\frac{i}{z_{Cu}F} \quad \text{for cupric ion ,} \tag{1}$$

$$vC_{Na}+\mu_{Na}EC_{Na}=vC^*_{Na} \quad \text{for sodium ion ,} \tag{2}$$

$$vC_{SO_4}-\mu_{SO_4}EC_{SO_4}=vC^*_{SO_4} \quad \text{for sulfate ion ,} \tag{3}$$

where v is the growth velocity, C_i and C_i^* ($i=$Cu,Na,SO_4) are the concentration of each ion in the bulk solution and inside the aggregate, and μ_i stands for the respective ionic mobilities. Additionally, E is the electric field and i is the current density. If C and C_{inert} represent, respectively, the concentration of copper sulfate and sodium sulfate, the relation between the concentration of inert electrolyte inside the aggregate and in the bulk solution is

$$C^*_{inert}=\left[1+\frac{\mu_{Na}E}{v}\right]C_{inert} \tag{4}$$

and the growth velocity v as a function of the bulk concentration of inert electrolyte is expressed by

$$v=\mu_{SO_4}E+\frac{(\mu_{Na}+\mu_{SO_4})E}{C}C_{inert} \ . \tag{5}$$

The growth velocity can be also expressed as a function of the conductivity of the electrolyte solution. Rewriting Eq. (5) in terms of individual ionic concentrations and considering that, in our case, the conductivity of the electrolyte solution κ is given by

$$\kappa=F(z_{SO_4}\mu_{SO_4}C_{SO_4}+z_{Cu}\mu_{Cu}C_{Cu}+z_{Na}\mu_{Na}C_{Na}) \ ,$$

the growth velocity reads

$$v=\frac{E\kappa}{z_{Cu}FC}(1-t_{Cu}) \ , \tag{6}$$

t_{Cu} being the transference number of copper ions.

Finally, the expression of the current density can be easily derived from Eq. (1), taking into account the value of growth velocity given by Eq. (5). In this case

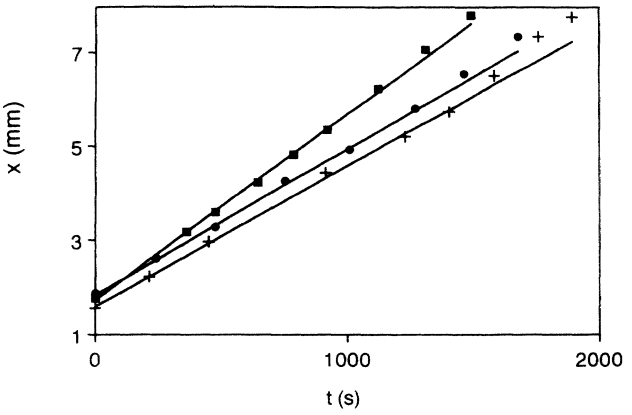

FIG. 8. Deposit height vs time dependences for homogeneous growth patterns. ●: $\Delta V=5$ V, $[Na_2SO_4]=1$ mM. +: $\Delta V=4$ V, $[Na_2SO_4]=12$ mM. ■: $\Delta V=7$ V, $[Na_2SO_4]=1$ mM.

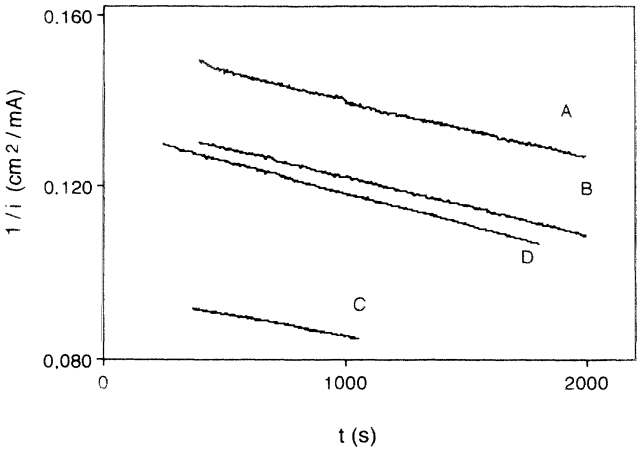

FIG. 9. Experimental i^{-1} vs time dependences for homogeneous growth patterns. *A*: $\Delta V=5$ V, $[Na_2SO_4]=3$ mM. *B*: $\Delta V=7$ V, $[Na_2SO_4]=2$ mM. *C*: $\Delta V=5$ V, $[Na_2SO_4]=8$ mM. *D*: $\Delta V=7$ V, $[Na_2SO_4]=3$ mM.

$$i=EF(z_{Cu}\mu_{Cu}C_{Cu}+z_{SO_4}\mu_{SO_4}C_{SO_4}+z_{Na}\mu_{Na}C_{Na})=\kappa E$$

and Ohm's law is obtained as can be expected from the assumptions of our model. Moreover, the temporal dependence of current density at constant applied potential ΔV is calculated from the relation between the electric field and the applied potential

$$i=\kappa\frac{\Delta V}{d-x}\ , \tag{7}$$

d being the electrode separation and x the deposit height. In our case, experimental results evidence that the growth velocity during the stage of development of homogeneous patterns may be taken as a constant (Fig. 8) [17]. As a matter of fact, this result is compatible with Eqs. (5) and (7), given the small extent of the whole electrode separation, i.e., $x<d$, over which stable homogeneous patterns can be analyzed. Then

$$\frac{1}{i}=\frac{1}{i_0}-\frac{v}{\kappa\Delta V}(t-t_0)\ , \tag{8}$$

where t_0 is the induction time and i_0 is the current density at the start of the Ohmic growth. Equation (8) states the condition for the dependence of current density vs time to be satisfied under the assumption of an Ohmic control of the homogeneous growth and constant velocity growth.

Equivalent forms of Eq. (6) above were previously derived by different groups in the absence of an inert electrolyte. Its validity, assuming an Ohmic control of the electrodeposition reaction, has been verified under different experimental conditions (radial and parallel cells, and at constant potential and at constant current) [9,12,16].

Moreover, if we analyze the particular case of a binary electrolyte, Eq. (5) shows that

$$v=\mu_{SO_4}E\ ,$$

indicating that, under these conditions, the velocity of the withdrawal of anions from the cathodic to the anodic region determines the growth velocity of the deposit. This condition was first assumed by Fleury *et al.* to explain the kinetics of homogeneous pattern formation in these conditions [9,15].

Our results indicate that the Ohmic model can be extended to a homogeneous growth from a solution containing the electroactive salt and small amounts of an inert electrolyte.

Figure 9 shows typical i^{-1} vs t plots, after the initial current transient regime (Fig. 6), for homogeneous patterns in zone III of the diagram of morphologies. We can observe a linear relation in good agreement with Eq. (8). In addition, growth velocities directly measured from temporal image analysis of experimental patterns also show a satisfactory agreement with those calculated from these plots (Table I). It is worth noting that the growth velocity of open fractal patterns (for instance, 1mM Na_2SO_4, 5 V; zone II of the diagram of morphologies), for which diffusion plays a more important role, is markedly smaller than that extrapolated from the Ohmic model. This behavior is also clearly seen in Figs. 10 and 11 where growth velocity is plotted against inert electrolyte concentration and solution conductivity, respectively, for different potential values.

Equation (5) shows that growth velocity of homogeneous patterns increases with inert electrolyte concentration, and that this dependence is also larger when the applied potential is increased. Taking ionic mobilities as constants in the electrolyte composition range studied, but corrected for our typical solution concentrations, and invoking the hypothesis above, i.e., $x<d$, $E\approx\Delta V/d$, this dependence may be taken as linear, with theoretical slopes equal to 0.20, 0.15, and 0.12 $\mu m\,s^{-1}\,mM^{-1}$ for 7, 5, and 4 V, respectively, at 0.05M $CuSO_4$.

In spite of the relative small extent of experimental conditions where Eq. (5) can be tested, we think that our experimental results reasonably agree with this behavior. Figure 10 shows the experimental dependences of growth velocities vs inert electrolyte concentration at 7, 5, and 4

TABLE I. Growth velocity values at several experimental conditions for the three-ion system. $[CuSO_4]=0.05M$. v_{expt}, experimental; v_{calc}, calculated from Eq. (8).

$[Na_2SO_4]$ (mM)	ΔV (V)	Morphology	V_{expt} ($\mu m\,s^{-1}$)	V_{calc} ($\mu m\,s^{-1}$)
6	4	Homogeneous	3.00	3.28
1	5	Open	1.19	2.43
2.5	5	Homogeneous	2.97	3.19
3	5	Homogeneous	3.26	3.50
4	5	Homogeneous	3.04	3.43
6	5	Homogeneous	3.12	4.00
8	5	Homogeneous	3.17	4.82
0.25	7	Homogeneous	3.58	3.34
2	7	Homogeneous	3.96	4.39
3	7	Homogeneous	4.33	4.41
3	7	Homogeneous	4.34	4.22

V and 0.05M $CuSO_4$. In this plot, growth velocity values have been averaged over several experiments in order to minimize errors due to the definition of the growing front. It is observed that the general trends predicted by Eq. (5) are fulfilled. A more detailed analysis of these results show that theoretical dependences are mostly attained at low values of inert electrolyte concentration (up to 4–5 mM Na_2SO_4). At 7 V, homogeneous deposits are formed up to 7mM Na_2SO_4, but the experimental slope (0.22 ± 0.03 $\mu m\,s^{-1}\,mM^{-1}$) is close to the expected value only up to 4 mM Na_2SO_4. At 5 V, homogeneous deposits are formed from 2 mM up to 8 mM Na_2SO_4, but a linear dependence with a slope 0.14 ± 0.04 $\mu m\,s^{-1}\,mM^{-1}$, which agrees with the theoretical value, is only obtained between 2–4 mM Na_2SO_4; at lower concentration values, open patterns are formed with smaller growth velocities, whereas at higher concentration, a slight decrease of growth velocities is also observed. At 4 V, homogeneous patterns are formed at larger inert electrolyte concentration, and the experimental slope is lower than the theoretical value. Finally, the ionic mobility of a sulfate anion calculated from experimental ordinates (2.07×10^{-4}, 2.17×10^{-4}, and 2.52×10^{-4} $cm^2\,V^{-1}\,s^{-1}$ at 7, 5, and 4 V, respectively) is somewhat smaller than the value for unsupported cupric sulfate solutions at 0.05M SO_4Cu, calculated from Miller *et al.* (2.95×10^{-4} $cm^2\,V^{-1}\,s^{-1}$ at 20 °C [11]. This could be attributed to the potential drop taking place at the interfaces [9], although our values for the slopes do not appear to be sensitive to this effect. A similar behavior of growth velocity in front of electrolyte conductivity according to Eq. (6) is also observed (Fig. 11).

V. ON THE ORIGIN OF THE FINGER PATTERN TEXTURE

The shape of the dividing line between homogeneous and finger patterns in the diagram of morphologies, similar to that of a hyperbola (Fig. 1), suggests that there exists a current density threshold in the crossover between both structures. This follows previous suggestions of different authors indicating that current density can be a more suitable parameter to classify the different morphologies of an electrodeposit [4–6,9].

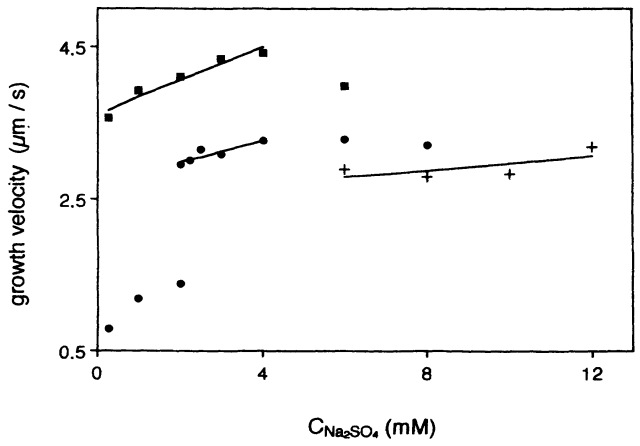

FIG. 10. Growth velocity of homogeneous electrodeposits plotted vs sodium sulfate concentration. ■: $\Delta V=7$ V. ●: $\Delta V=5$ V. +: $\Delta V=4$ V.

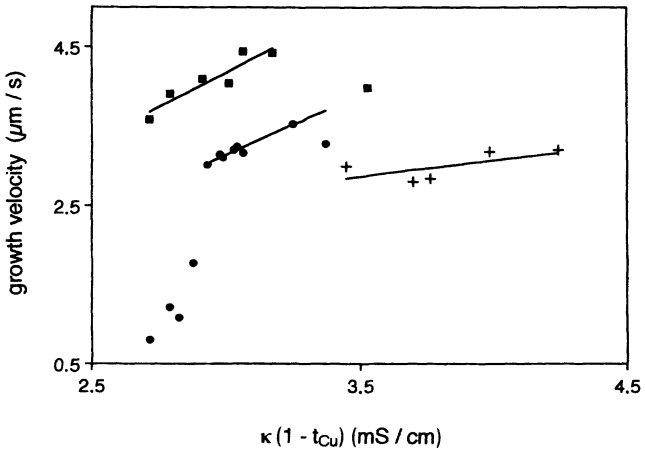

FIG. 11. Growth velocity of homogeneous electrodeposits plotted vs electrolyte solution conductivity. ■: $\Delta V=7$ V. ●: $\Delta V=5$ V. +: $\Delta V=4$ V.

In our case, at the first stages of the electrodeposit growth, there is a constant relation between applied potential and electric field through the initial electrode separation. Moreover, assuming a dilute solution behavior, the concentration of inert electrolyte is linearly related to the solution conductivity, and therefore

$$i=\kappa E \simeq (a+bC_{\text{inert}})\frac{\Delta V}{d} , \tag{9}$$

where

$$a=2FC(\mu_{SO_4}+\mu_{Cu}) ,$$

$$b=2F(\mu_{SO_4}+\mu_{Na}) .$$

Thus, Eq. (9) above is consistent with a current density threshold selecting between homogeneous and finger patterns in copper electrodeposition under our experimental conditions. This distinctive role of the current density may be further justified by referring to the eventual competition between copper electrodeposition and other electrochemical reactions, which can take place at large current density values. Actually, hydrogen evolution must be considered as the first electrochemical reaction accompanying copper electrodeposition at large inert electrolyte concentration and applied potential values. Recently, the role of dissolved oxygen reduction has also been reported [18].

This behavior might be connected with other features of both morphologies: (i) the different aspect and color of both deposits, metallic and red for homogeneous and nonmetallic and dark grey for finger patterns; and (ii) the current decrease during the dynamical transition from homogeneous to finger patterns, or the opposite behavior (current increase) during the dynamical transition from finger to homogeneous deposits. Hydrogen evolution follows the reduction path

$$2H_2O+2e^- \rightarrow H_2+2OH^- \tag{10}$$

leading to a local *p*H increase in the electrolyte solution close to the electrode surface. A similar behavior could also be expected in the case of oxygen reduction. As a first consequence, this would induce the precipitation of copper oxygenated species jointly with the electrodeposition of copper, resulting in the formation of a less metallic deposit with a dark grey color. The current decrease in the transition from homogeneous to finger patterns would account for the conductivity diminution of the finger deposit due to its partial nonmetallic nature.

However, other processes should be also taken into account in the basic solution surrounding the electrode surface. Among them, we have to consider the reduction of copper cation to cuprous oxide [19], through either a pure electrochemical path

$$2Cu^{2+}+2OH^-+2e^- \rightarrow Cu_2O+H_2O$$

or a chemical reaction involving the newly formed hydrogen

$$2Cu^{2+}+H_2+4OH^- \rightarrow Cu_2O+3H_2O .$$

These reactions also imply the formation of a partially nonmetallic deposit. Finally, the formation of interstitial solid solutions of hydrogen in copper and of copper hydride during hydrogen evolution has also been reported in the literature [20,21].

As a final observation, notice that the dynamic transition from homogeneous to finger patterns observed in zone III of the diagram of morphologies is consistent with this assumption, since the electric field in the growing front (and subsequently, the current density) increases as the deposit grows.

VI. CONCLUSIONS

The morphology of copper electrodeposits, obtained from a nondeaerated copper sulfate aqueous solution, is clearly influenced by the presence of an inert electrolyte (sodium sulfate) in the solution. Apart from the morphological change of the deposit after small additions of inert electrolyte, the most interesting feature is the fingerlike morphology observed at high applied potential and inert electrolyte concentration values. We conjecture that this new morphology is formed as a result of concurrent electrode reactions taking place together with copper electrodeposition, when a current density threshold is attained. Apart from the chemical considerations that would explain some of the observations (composition, color, etc), it is obvious that other morphological features of this growth mode might be interpreted by referring to more pure physical phenomena as screening effects in the transport mechanism [22], diminution of the deposit conductivity [23], surface tension or hydrodynamic effects in the interface between the bulk solution and the concentration layer [24,25], etc. More work is now in progress to clearly elucidate this structure.

Moreover, our growth velocity measurements of homogeneous patterns in the presence of an inert electrolyte in solution satisfactorily agree with a theoretical model based on a migration transport regime of electroactive species from the bulk solution to the electrode surface. Growth velocities are linear with respect to inert electrolyte concentration mainly at low values, except when open fractal structures are formed; in this case, the growth velocity is clearly smaller than the calculated one from this model. At higher inert electrolyte concentration values, the measured growth velocities are smaller than the theoretical ones, probably due to an incipient contribution of the electrochemical processes giving rise to fingerlike patterns.

ACKNOWLEDGMENTS

We are grateful to Dr. D. P. Barkey for fruitful discussions. One of us (P.P.T.) benefited from financial support from the Ministerio de Educación y Ciencia, Spain. Financial support from the Dirección General de Investigación Científica y Tecnológica (DGICYT), Spain, under Project No. PB90-0455, and the Comissió Interdepartamental de Recerca i Innovació Tecnològica de la Generalitat de Catalunya (CIRIT), Catalonia, Spain, is acknowledged.

[1] L. M. Sander, in *The Physics of Structure Formation,* edited by W. Guttinger and G. Dangelmayr (Springer, Berlin, 1987), p. 257.
[2] D. A. Kessler, J. Koplik, and H. Levine, Adv. Phys. **37**, 255 (1988).
[3] Y. Sawada, A. Dougherty, and J. P. Gollub, Phys. Rev. Lett. **56**, 1260 (1986).
[4] D. G. Grier, E. Ben-Jacob, R. Clarke, and L. M. Sander, Phys. Rev. Lett. **56**, 1264 (1986).
[5] P. P. Trigueros, J. Claret, F. Mas, and F. Sagués, J. Electroanal. Chem. **312**, 219 (1991).
[6] P. P. Trigueros, J. Claret, F. Mas, and F. Sagués, J. Electroanal. Chem. **328**, 165 (1992).
[7] G. L. M. K. S. Kahanda and M. Tomkiewicz, J. Electrochem. Soc. **136**, 1497 (1989).
[8] M. A. Guzman, R. D. Freimuth, P. U. Pendse, M. C. Veinott, and L. Lam, in *Nonlinear Structures in Physical Systems,* edited by L. Lam and H. Morris (Springer, New York, 1990), p. 32.
[9] V. Fleury, M. Rosso, J. N. Chazalviel, and B. Sapoval, Phys. Rev. A **44**, 6693 (1991).
[10] J. O.'M. Bockris and A. K. N. Reddy, *Modern Electrochemistry* (Plenum, New York, 1977), Vol. 1.
[11] D. G. Miller, J. A. Rard, L. B. Epstein, and R. A. Robinson, J. Solution Chem. **9**, 467 (1980).
[12] J. R. Melrose, D. B. Hibbert, and R. C. Ball, Phys. Rev. Lett. **65**, 3009 (1990).
[13] P. Garik, D. Barkey, E. Ben-Jacob, E. Bochner, N. Broxholm, B. Miller, B. Orr, and R. Zamir, Phys. Rev. Lett. **62**, 2703 (1989).
[14] V. Fleury, M. Rosso, and J. N. Chazalviel, Phys. Rev. A **43**, 6908 (1991).
[15] V. Fleury, J. N. Chazalviel, M. Rosso, and B. Sapoval J. Electroanal. Chem. **290**, 249 (1990).
[16] D. Barkey, P. Garik, E. Ben-Jacob, B. Miller, and B. Orr, J. Electrochem. Soc. **139**, 1044 (1992).
[17] The apparent contradiction in Eq. (6) between a constant growth velocity and an increasing current density might be preliminarily related to the partially nonmetallic nature of the copper homogeneous deposit in presence of sodium sulfate, as evidenced by our recent findings after submission of this manuscript. This fact, associated with concurrent reactions additional to pure Cu^{2+} reduction, would affect the resistivity of the deposit and the actual meaning of the current density in the model.
[18] A. Kuhn and F. Argoul, Fractals **1**, 451 (1993).
[19] F. A. Cotton and G. Wilkinson, *Advanced Inorganic Chemistry* (Wiley, New York, 1966).
[20] S. Nakahara and Y. Okinaka, Script. Met. **19**, 517 (1985).
[21] L. Burzynska, Z. Zembura, and J. Karp, React. Solids **7**, 409 (1989).
[22] E. Louis, F. Guinea, O. Pla, and L. M. Sander, Phys. Rev. Lett. **68**, 209 (1992).
[23] C. P. Chen and J. Jorné, J. Electrochem. Soc. **137**, 2047 (1990).
[24] D. Barkey, J. Electrochem. Soc. **138**, 2912 (1991).
[25] P. Garik, J. Hetrick, B. Orr, D. Barkey, and E. Ben-Jacob, Phys. Rev. Lett. **66**, 1606 (1991).

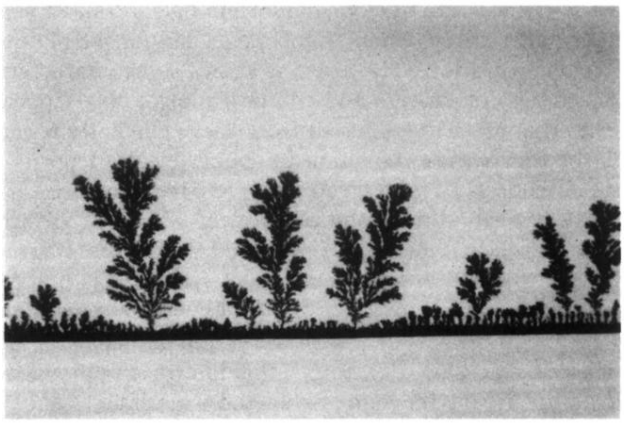

FIG. 2. Open fractal copper electrodeposit corresponding to zone II of the diagram of morphologies. The width of the picture corresponds to 23 mm. $\Delta V = 5$ V, $[Na_2SO_4] = 1$ mM.

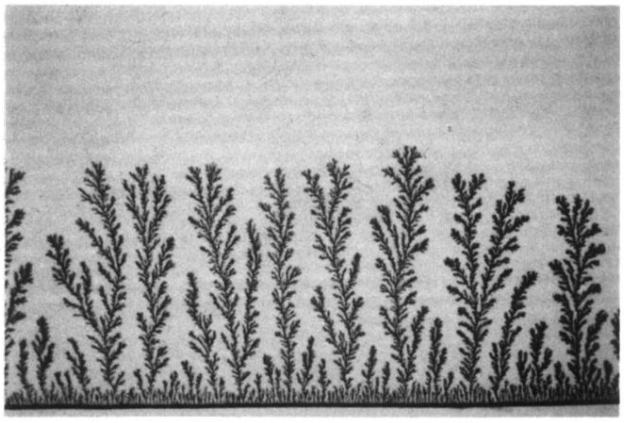

FIG. 3. Homogeneous copper electrodeposit corresponding to zone III of the diagram of morphologies. The width of the picture corresponds to 23 mm. $\Delta V = 5$ V, $[Na_2SO_4] = 4$ mM.

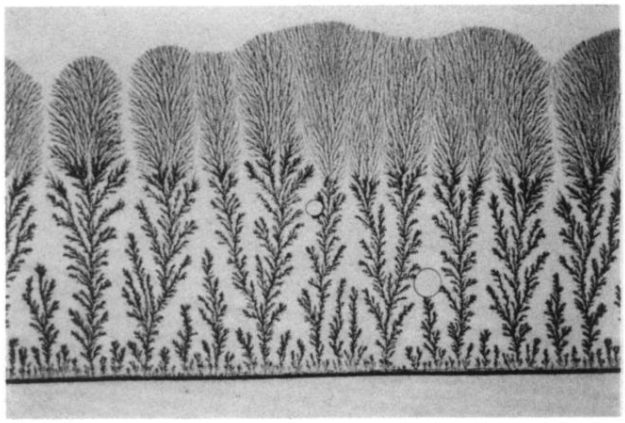

FIG. 4. Complex pattern showing the dynamical transition from a homogeneous structure to a fingerlike texture. Notice that the fine structure of the first part of the deposit is the same as that of the fingerlike morphology. The width of the picture corresponds to 23 mm. $\Delta V = 5$ V, $[Na_2SO_4] = 6$ mM.

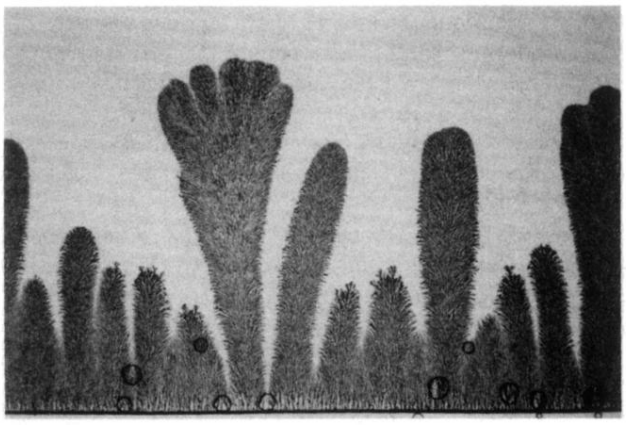

FIG. 5. Fingerlike copper electrodeposit corresponding to zone IV of the diagram of morphologies. The width of the picture corresponds to 23 mm. $\Delta V = 25$ V, $[Na_2SO_4] = 2$ mM.